A simple approximation to the electron-phonon interaction in population dynamics

Carlos M. Bustamante,[1, a)] Tchavdar N. Todorov,[2, b)] Cristian G. Sánchez,[3] Andrew Horsfield,[4] and Damian A. Scherlis[1, c)]

[1)] *Departamento de Química Inorgánica, Analítica y Química Física/INQUIMAE, Facultad de Ciencias Exactas y Naturales, Universidad de Buenos Aires, Buenos Aires (C1428EHA) Argentina*

[2)] *Atomistic Simulation Centre, School of Mathematics and Physics, Queen's University Belfast, Belfast BT7 1NN, United Kingdom*

[3)] *Instituto Interdisciplinario de Ciencias Básicas, Facultad de Ciencias Exactas y Naturales, Universidad Nacional de Cuyo, CONICET, Padre Jorge Contreras 1300, Mendoza M5502JMA, Argentina*

[4)] *Department of Materials, Thomas Young Centre, Imperial College London, South Kensington Campus, London, SW7 2AZ, United Kingdom*

The modelling of coupled electron-ion dynamics including a quantum description of the nuclear degrees of freedom has remained a costly and technically difficult practice. The Kinetic Model for electron-phonon interaction provides an efficient approach to this problem, for systems evolving with low amplitude fluctuations, in a quasi-stationary state. We propose in this work an extension of the Kinetic Model to include the effect of coherences, which are absent from the original approach. The new scheme, referred to as Liouville von Neumann - Kinetic Equation (or LvN+KE), is implemented here in the context of a tight-binding Hamiltonian and employed to model the broadening, caused by the nuclear vibrations, of the electronic absorption bands of an atomic wire. The results, which show close agreement with the predictions given by Fermi's Golden Rule, serve as a validation of the methodology. Thereafter, the method is applied to the electron-phonon interaction in transport simulations, adopting to this end the driven Liouville von Neumann equation to model open quantum boundaries. In this case the LvN+KE model qualitatively captures the Joule heating effect and Ohm's law. It however exhibits numerical discrepancies with respect to the results based on Fermi's Golden Rule, attributable to the fact that the quasi-stationary state is defined taking into consideration the eigenstates of the closed system rather than those of the open boundaries system. The simplicity and numerical efficiency of this approach and its ability to capture the essential physics of the electron-phonon coupling make it an attractive route to first-principles electron-ion dynamics.

[a)]Electronic mail: cbustamante@qi.fcen.uba.ar

[b)]Electronic mail: t.todorov@qub.ac.uk

[c)]Electronic mail: damian@qi.fcen.uba.ar

I. INTRODUCTION

The description of the coupling between the electronic and the ionic vibrational degrees of freedom, or the electron-phonon interaction, turns out to be essential for the quantum-mechanical modelling of molecules and materials at finite temperature.[1] The effect of the atomic vibrations on the electronic structure, and vice versa, manifests in all physical properties from spectroscopy to energy transfer and conductivity. A well known example of interest to the present study is Joule heating,[2,3] originating in the flow of electrons through a conductor. As the electrons are scattered by the ions, part of their energy is absorbed by the ionic vibrations. This effect is also responsible for the electrical resistivity of the conductor and its temperature dependence. The quantum-mechanical description of Joule heating is a challenging endeavor that has been the focus of continuous research extending over decades.[4–15]

The electron-phonon coupling in atomistic descriptions can be addressed either within a static picture, typically on the basis of perturbation theory,[1,16–18] or in an explicitly time-dependent framework through molecular dynamics simulations. The latter are most often implemented semiclassically, solving the Newton equations for the nuclei subject to the forces arising from the quantum-mechanical electronic Hamiltonian.[19–24] Molecular dynamics simulations can be performed adiabatically—meaning that the evolution of the system is restrained to a single electronic state or potential energy surface—via the Born-Oppenheimer approximation or the Car-Parrinello method; or non-adiabatically, where the most usual schemes are Ehrenfest and surface hopping dynamics.[19,21,22] In Ehrenfest dynamics ions and electrons are propagated classically and quantum-mechanically respectively, interacting with each other as time-dependent mean fields. Because of this averaged interaction, the

formalism fails at describing the phonon emission produced by electronic deexcitation, due to the lack of electron-ion correlation. This also affects the thermodynamic equilibration of the system as the electrons cannot transfer kinetic energy to the ions. In particular the forces on the nuclei given by the mean-field potential might not correspond to a specific energy surface but to a combination, since the electronic wavefunction reflects a mixed quantum population. As a consequence, when the system evolves in a region where two or more potential energy surfaces are close in energy, the Ehrenfest method can lead to unphysical trajectories not corresponding to a well defined quantum state.[20–22] In the surface hopping technique, on the other hand, the dynamics proceeds on a specific electronic surface, and once every few steps the probabilities associated with transitions to the closest states are assessed, to let the system jump to another surface according to such probabilities. This method cures some of the deficiencies of the Ehrenfest scheme, but exhibits its own limitations: only very few electronic states can be considered in practice, and it tends to misrepresent decoherence.[24]

In order to go beyond these semiclassical treatments, Correlated Electron-Ion Dynamics (CEID)[25,26] was developed by Horsfield et al. This formulation solves the electron-nuclear quantum Hamiltonian approximately adopting a perturbative expansion in powers of nuclear fluctuations about the mean trajectory. Its success is to describe non-adiabatic phenomena; its main limitation is its scaling with the number of moving atoms. This issue was partially alleviated by the so called Effective Correlated Electron-Ion Dynamics (ECEID),[11] that improves the scaling of CEID by focusing on the case of harmonic potentials. This formalism shows a good description of thermal equilibration between electrons and phonons, and electronic transport in open systems.[27] Nevertheless, it is still expensive for an *ab initio* setting such as DFT, and even more in the context of transport calculations.

Efforts have gone into the development of nonadiabatic molecular dynamics through the

calculation of current-induced forces or electronic friction.[28–34] Many of these treatments exhibit a great generality and are applicable to nonequilibrium open quantum systems, although they have been typically implemented in the context of multi-level systems coupled to a few vibrational modes, rather than in explicit atomistic frameworks.

For closed systems and using a harmonic potential, the situation can be simplified by the kinetic model (KM),[11,26] an approximation based on lowest-order perturbation theory. We note that this is similar to procedures used in semiconductor optics.[35,36] The main physical assumption of the KM, which is at the same time one of its major limitations, is to consider that the electron-phonon system remains close to an instantaneous stationary state, preserving the eigenvalues while evolving only the occupancies. This simplification entails the suppression of the coherences, but in return it shows several strengths: flexibility in the choice of the unperturbed electronic Hamiltonian, the vibrational modes, and the coupling between the two systems, and of couse the computational tractability. With the purpose of exploiting the simplicity of KM, we present in this work an *ad hoc* master equation grounded in this model. This new formulation corrects the lack of electron coherence exhibited by the original approach and overcomes some of its limitations. In Section II we introduce the KM formalism and its *ad hoc* extension leading to the present equation of motion. In Section III we apply this formalism to study the effect of the phonon temperature on the electronic spectrum of a linear molecule described with a tight-binding model, and compare the results with the predictions of Fermi's Golden Rule (FGR). Finally, in Section IV we show how these equations can be used to investigate the effect of electron-phonon interactions in transport dynamics under a bias with electronic open boundaries.

II. THE KINETIC MODEL AND INCLUSION OF COHERENCE IN THE EQUATION OF MOTION

The KM is developed starting from a Hamiltonian which considers the phonons as quantum harmonic oscillators and a phonon-electron interaction term which neglects the correlation between phonons:[26]

$$H = \sum_{\alpha} E_{\alpha} c_{\alpha}^{\dagger} c_{\alpha} + \sum_{j} \hbar\omega_j (a_j^{\dagger} a_j + 1/2) - \sum_{\alpha\beta j} \sqrt{\frac{\hbar}{2M\omega_j}} F_{\alpha\beta j} c_{\alpha}^{\dagger} c_{\beta} (a_j^{\dagger} + a_j). \tag{1}$$

In the above equation $\{c_\alpha\}$ are a set of fermion annihilation operators corresponding to the eigenstates $|\alpha\rangle$ of a chosen one-electron Hamiltonian H_e with eigenenergies E_α, while $\{a_j\}$ are boson annihilation operators for a set of vibrational modes with angular frequencies $\{\omega_j\}$. M is the oscillator mass. The matrix elements $F_{\alpha\beta j}$ can be obtained from an explicitly chosen electron-phonon coupling. Here we adopt the relation

$$F_{\alpha\beta j} = -\langle\alpha|\frac{\partial H_e}{\partial X_j}|\beta\rangle, \tag{2}$$

where X_j is the generalized displacement for the vibrational mode j. Under the assumption that the density matrix ρ always commutes with the unperturbed Hamiltonian, i.e. the dynamics does not alter the eigenvalues of the system but only the populations, perturbation theory to the lowest-order can be used to express the occupancy variation rate of the electronic state α as[26]

$$\frac{\partial \rho_\alpha}{\partial t} = -\eta_\alpha \rho_\alpha + \Lambda_\alpha \tag{3}$$

where

$$\eta_\alpha = \sum_{\beta j} \frac{\pi}{M\omega_j} |F_{\alpha\beta j}|^2 [(N_j + \rho_\beta)\delta(E_\alpha - E_\beta + \hbar\omega_j) + (N_j - \rho_\beta + 1)\delta(E_\alpha - E_\beta - \hbar\omega_j)], \tag{4}$$

$$\Lambda_\alpha = \sum_{\beta j} \frac{\pi}{M\omega_j} |F_{\alpha\beta j}|^2 \rho_\beta [(N_j + 1)\delta(E_\alpha - E_\beta + \hbar\omega_j) + N_j \delta(E_\alpha - E_\beta - \hbar\omega_j)], \tag{5}$$

with N_j the population of phonon mode j. The inverse lifetime η_α is related to the imaginary part of the retarded electronic self-energy correction due to phonons.[37,38] Equation 3 will be henceforth called the kinetic equation (KE). Here, and unless otherwise specified, the Hamiltonian and density matrix are expressed in the eigenstate basis. For the occupancy variation rate of the vibrational mode j we obtain

$$\dot{N}_j = \frac{2\pi}{\hbar}\sum_{\alpha\beta}\frac{\hbar}{2M\omega_j}|F_{\alpha\beta j}|^2[-\rho_\alpha(1-\rho_\beta)N_j + \rho_\beta(1-\rho_\alpha)(N_j+1)]\delta(E_\alpha - E_\beta + \hbar\omega_j). \quad (6)$$

Equation (3) conserves particle number, $\sum_\alpha \dot{\rho}_\alpha = 0$, while (3) and (6) conserve the total energy $E = \sum_\alpha \rho_\alpha E_\alpha + \sum_j (N_j + 1/2)\hbar\omega_j$.

Practical implementations in finite systems with discrete levels incorporate the energy-conserving delta functions above in the form of a normalized narrowly peaked function of finite width, for example:

$$\delta(E_\alpha - E_\beta \pm \omega_j\hbar) \approx \frac{1}{\sqrt{2\pi\sigma^2}} e^{\frac{-(E_\alpha - E_\beta \pm \hbar\omega_j)^2}{2\sigma^2}}. \quad (7)$$

With this approximation the particle number remains identically conserved, but the other properties above can be violated.[39] A way to enforce total energy conservation is to replace (6) by

$$\dot{N}_j = \frac{2\pi}{\hbar}\sum_{\alpha\beta}\frac{\hbar}{2M\omega_j}|F_{\alpha\beta j}|^2[-\rho_\alpha(1-\rho_\beta)N_j + \rho_\beta(1-\rho_\alpha)(N_j+1)]\left(\frac{E_\beta - E_\alpha}{\hbar\omega_j}\right)\frac{\exp\left(\frac{-(E_\alpha - E_\beta + \hbar\omega_j)^2}{2\sigma^2}\right)}{\sqrt{2\pi\sigma^2}}. \quad (8)$$

The parameter σ must be of the order of the lowest electronic energy difference. Its value can be calibrated by fixing the population of phonons (electrons) to function as a thermal bath for the electrons (phonons) initially at a different temperature, and seeking thermal equilibration between the two subsystems. In the Appendix this procedure is applied to identify the optimal value of σ for the parameters used in the calculations of Sections III and IV.

In what follows, we present an heuristic extension of the KE to include coherences. To do so, we note that, providing that the density matrix ρ commutes with the electronic Hamiltonian (quasi-stationary condition), we can consider the Liouville von Neumann (LvN) equation and rewrite equation (3) as:

$$\frac{\partial \rho}{\partial t} = \frac{1}{\mathrm{i}\hbar}[H_e, \rho] - \begin{bmatrix} \eta_1\rho_{11} - \Lambda_1 & 0 & \cdots & 0 \\ 0 & \eta_2\rho_{22} - \Lambda_2 & \cdots & 0 \\ \vdots & \vdots & \ddots & \vdots \\ 0 & 0 & \cdots & \eta_N\rho_{NN} - \Lambda_{NN} \end{bmatrix}. \tag{9}$$

where we replaced the notation of ρ_α by $\rho_{\alpha\alpha}$ since we are now working with electronic occupations as elements of the density matrix. In this expression the coherences can be incorporated in an *ad hoc* fashion as the arithmetic mean of the diagonal terms. This somehow intuitive construction leads to the LvN+KE equation of motion:

$$\frac{\partial \rho}{\partial t} = \frac{1}{\mathrm{i}\hbar}[H_e, \rho] - \begin{bmatrix} \eta_1\rho_{11} - \Lambda_1 & \frac{\eta_1+\eta_2}{2}\rho_{12} & \cdots & \frac{\eta_1+\eta_n}{2}\rho_{1N} \\ \frac{\eta_2+\eta_1}{2}\rho_{21} & \eta_2\rho_{22} - \Lambda_2 & \cdots & \frac{\eta_2+\eta_N}{2}\rho_{2N} \\ \vdots & \vdots & \ddots & \vdots \\ \frac{\eta_N+\eta_1}{2}\rho_{N1} & \frac{\eta_N+\eta_2}{2}\rho_{N2} & \cdots & \eta_N\rho_{NN} - \Lambda_N \end{bmatrix}. \tag{10}$$

The form of this equation can be motivated by the damped evolutionary operator U defined by the ansatz:

$$U|\alpha\rangle = e^{-\mathrm{i}(E_\alpha/\hbar - \mathrm{i}\gamma_\alpha)t}|\alpha\rangle \tag{11}$$

where $|\alpha\rangle$ is an eigenstate of the unperturbed Hamiltonian. According to this, it is possible to write the density matrix elements as function of time as

$$\langle\alpha|U\rho(0)U^\dagger|\alpha\rangle = e^{-2\gamma_\alpha t}\rho_{\alpha\alpha}(0), \tag{12}$$

$$\langle\alpha|U\rho(0)U^\dagger|\beta\rangle = e^{-\mathrm{i}((E_\alpha - E_\beta)/\hbar - \mathrm{i}(\gamma_\alpha+\gamma_\beta))t}\rho_{\alpha\beta}(0). \tag{13}$$

Under these considerations, the off-diagonal elements of the density matrix are affected by the average damping of the diagonal terms. Similar ideas have been already reported based on FGR[40] or semi-empirical methodologies.[41]

Phonon coherences are not taken into account in the present work. In the simplest case of a single oscillator, they are measured by the quantity C^{PR} in equation 36 of ref. [26], in turn driven by the imbalance between ionic kinetic and potential energy. They are reflected also in time-variations in the quantity $\bar{R}$ defined in the same reference. Thus they would become important in highly non-stationary situations, different from the scenarios relevant to this study.

Variations of our formalism are present in other contexts concerning the quantum kinetics of semiconductors. In particular, a connection can be recognized with the so-called optical Bloch equations, and with the semiconductor Bloch equations—a generalization of the former that incorporate Coulomb interactions—which describe the density matrix dynamics coupled to a classical field $\vec{E}(\vec{r},t)$.[35,36] For a two-band system, the optical Bloch equations can be expressed as

$$\hbar\frac{\partial\rho}{\partial t} =$$

$$= \begin{bmatrix} -2\ \mathrm{Im}[\vec{E}(\vec{r},t)\cdot\vec{\mu}_{12}\cdot\rho_{12}] - \hbar\gamma_1(\rho_{11}-\rho_{11}^0) & i(E_1-E_2)\rho_{12} - i\vec{\mu}_{21}\cdot\vec{E}(\vec{r},t)\cdot(\rho_{22}-\rho_{11}) - \hbar\gamma_2\rho_{12} \\ -i(E_1-E_2)\rho_{21} + i\vec{\mu}_{12}\vec{E}(\vec{r},t)(\rho_{22}-\rho_{11}) - \hbar\gamma_2\rho_{21} & -2\ \mathrm{Im}[\vec{E}(\vec{r},t)\cdot\vec{\mu}_{21}\cdot\rho_{21}] + \hbar\gamma_1(\rho_{22}-\rho_{22}^0) \end{bmatrix}$$

where $\vec{\mu}_{12}$ is the transition dipole, E_n are the eigenvalues, ρ_{11}^0 and ρ_{22}^0 are equilibrium or ground state distributions, and γ_j are phenomenological damping rates[35] (it must be noted that in the semiconductor description the eigenvalues and the density matrix elements are functions of the wave vector $\vec{k}$, e.g., $\rho_{ij} = \rho_{ij}(\vec{k})$; this dependence was omitted in the equation above for conciseness). The structure of this dynamical equation is reminiscent of

our formulation, equation 10, in the sense that the evolution of the density matrix diagonal and off diagonal elements, also called occupations and transition amplitudes in the context of the Bloch equations, are determined by a damping rate multiplied by the same diagonal and off-diagonal elements, respectively. In the optical or semiconductor Bloch equations these damping parameters, whose microscopic origin is rationalized in the textbook by Schaefer and Wegener,[35] express the relaxation of an arbitrary distribution toward equilibrium. In equation 10 of our approach, η_1, η_2, and their arithmetic mean, defined in terms of the electron-phonon coupling $F_{\alpha\beta j}$, govern the dissipation rate in lieu of the phenomenological γ_j parameters.

III. SPECTROSCOPIC TESTS

In this Section we investigate the ability of LvN+KE to describe the effect of temperature on the electronic spectrum of a molecule. To this end quantum dynamics simulations were performed on a linear atomic chain of 120 atoms, employing a nearest-neighbor orthogonal tight-binding (TB) model with a hopping integral of -1 eV. All atoms, except the two at each end, are treated as Einstein oscillators (EO),[42,43] with mass 15 amu and frequencies randomly distributed in the interval 0.05 - 0.2 eV/$\hbar$. The coupling operator for the oscillator at site j, $F_j = -\frac{\partial H_e}{\partial X_j}$, in first quantized form reads[11]

$$F_j = C\left(|j\rangle\langle j-1| + |j-1\rangle\langle j| - |j+1\rangle\langle j| - |j\rangle\langle j+1|\right) \tag{14}$$

where C is the coupling parameter, set here to -1.0 eV/. The phonon populations were kept constant throughout the simulations ($\dot{N}_j(t) = 0$), so that they behave as a fixed temperature thermal bath. To initialize the dynamics the density matrix was perturbed through a phase

factor:

$$\rho_{ij} \rightarrow \rho_{ij} e^{\mathrm{i}\theta(x_i - x_j)} \tag{15}$$

where θ is an impulse and x_j is the position of atom j. This furnishes the electrons with a coherent velocity field triggering the evolution of the dipole moment.[44] With θ sufficiently small, and allowing the system to evolve in the absence of external perturbations, the time-dependence of the dipole moment turns out to be

$$\langle \mu(t) \rangle = \mathrm{i}e\theta \mathrm{Tr}\left\{U^\dagger[\rho, x]U\, x\right\} = \mathrm{i}e\theta \sum_{\alpha,\beta} x_{\alpha\beta} x_{\beta\alpha} (\rho_{\alpha\alpha} - \rho_{\beta\beta}) e^{\mathrm{i}\,\omega_{\alpha\beta} t} \tag{16}$$

where e is the electron charge, U is the evolution operator, x is the position operator and $\omega_{\alpha\beta} = (E_\alpha - E_\beta)/\hbar$. To introduce the effect of electron-phonon dissipation, equation (16) can be rewritten with the incorporation of a small exponential damping. As a matter of fact, to extract the spectrum from electron dynamics simulations with fixed nuclei, a damping factor γ is often included in the post-processing to model the finite lifetime of the electronic states.[45,46] With this amendment the dipole moment reads

$$\langle \mu(t) \rangle = \mathrm{i}e\theta \sum_{\alpha,\beta} x_{\alpha\beta} x_{\beta\alpha} (\rho_{\alpha\alpha} - \rho_{\beta\beta}) e^{\mathrm{i}(\omega_{\alpha\beta} - \gamma)t}, \tag{17}$$

whose Fourier transform provides the absorption spectrum:

$$\langle \mu(\omega) \rangle = -e\theta \sum_{\alpha,\beta} x_{\alpha\beta} x_{\beta\alpha} \frac{\mathrm{i}}{\mathrm{i}(\omega_{\alpha\beta} + \omega) - \gamma} (\rho_{\alpha\alpha} - \rho_{\beta\beta}), \tag{18}$$

$$\mathrm{Im}\, \langle \mu(\omega) \rangle = e\theta \sum_{\alpha,\beta} x_{\alpha\beta} x_{\beta\alpha} \frac{\gamma}{(\omega_{\alpha\beta} + \omega)^2 + \gamma^2} (\rho_{\alpha\alpha} - \rho_{\beta\beta}). \tag{19}$$

This shows that the absorption bands will consist of Lorentzian peaks with areas proportional to $|x_{\alpha\beta}|^2$, and widths given by the decay rate, or γ.

The results of our simulations are shown in Figure 1. Panel A depicts the temporal evolution of the dipole moment for different temperatures. It can be seen that the dipole

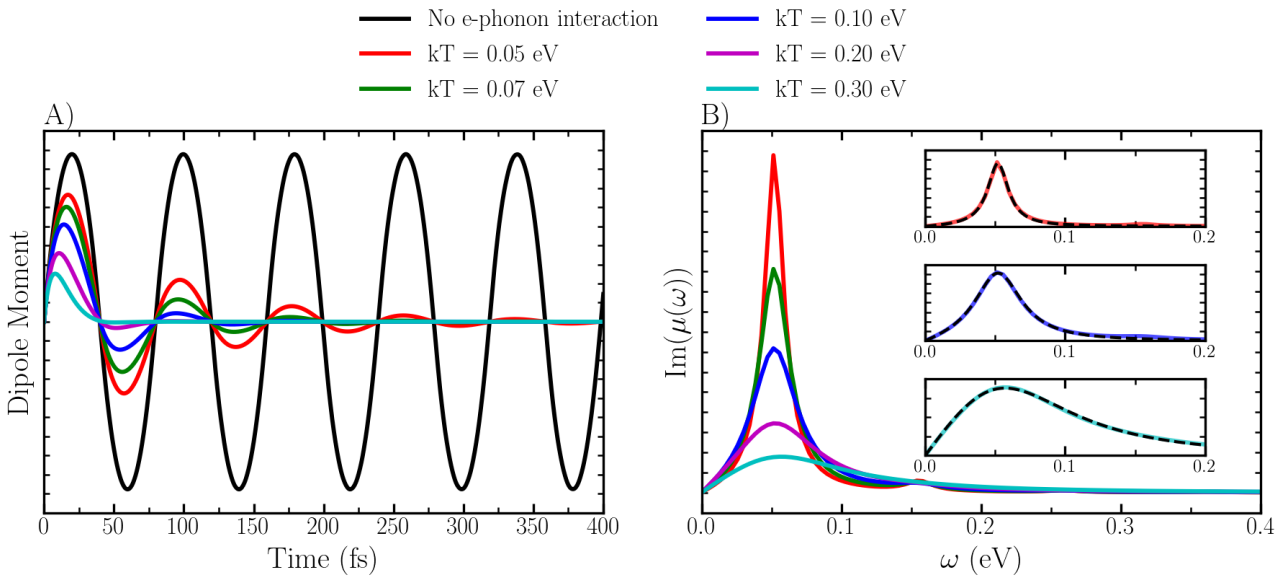

FIG. 1. A) Dipole moment of a linear molecule as a function of time, obtained in the absence of electron-phonon interaction and in its presence at different temperatures. B) Absorption spectrum corresponding to the curves shown in A. The insets present the fittings of equation (19) (dotted lines), to the simulated profiles.

oscillations are quenched by the energy exchange with the phonons, at a rate that depends on temperature: the higher the ionic kinetic energy, the larger the electron-ion scattering. The corresponding absorption spectra, computed as the imaginary part of the Fourier transform of the dipole moment, are presented on panel B. The damping factor γ can be estimated for each temperature by fitting equation (19) to the simulated spectra. These fittings are featured in the insets of Figure 1B.

The magnitude of the damping term can be assessed for an infinite chain from FGR. The back-scattering decay time τ_{bs} for a plane wave with momentum ψ scattered by a potential V is given by:

$$\frac{1}{\tau_{bs}} = \frac{2\pi}{\hbar} D(E) \langle |\langle -\psi | V | \psi \rangle|^2 \rangle_T \tag{20}$$

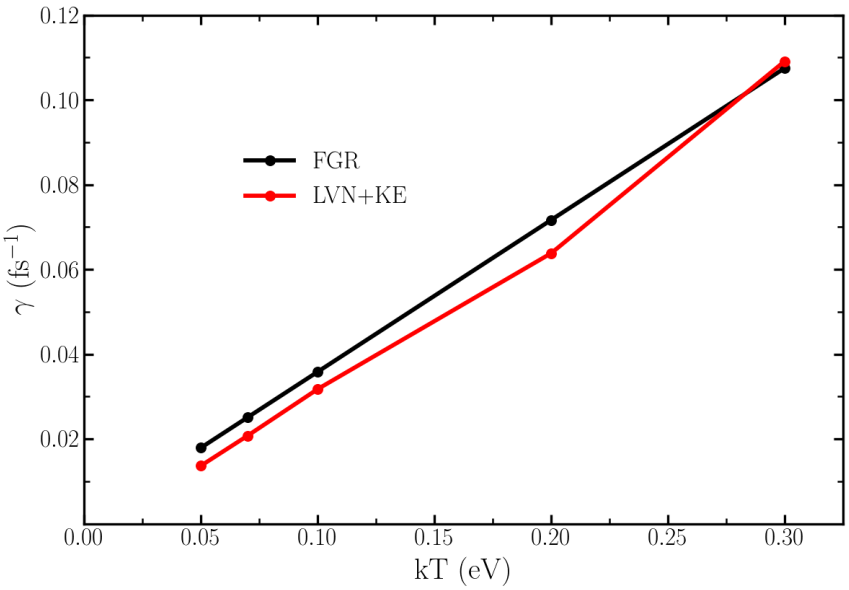

FIG. 2. Damping factor γ corresponding to the electron-phonon coupling obtained from LvN+KE simulations at various temperatures (red), and predicted by the Fermi golden rule (black).

where $D(E)$ is the density of states and $\langle\ \rangle_T$ denotes the thermal average. For the potential implicit in equation (1), $V = -\sum_{j=1} X_j F_j$, and considering transitions near the Fermi level, taken to be at the centre of the energy band, the following approximation is found in the regime $kT \gtrsim \hbar\omega$:

$$\frac{1}{\tau_{bs}} \approx \frac{C^2}{\hbar b} \frac{8 k_B T}{M \omega_1 \omega_2} \tag{21}$$

with b the hopping integral, and ω_1 and ω_2 the upper and lower limits for the random distribution of oscillator frequencies used in the calculations. According to equation (21) the broadening of the spectral peaks has a linear dependence on temperature. Figure 2 presents the widths of the bands predicted by this equation, compared with those corresponding to the Lorentzian fittings of Figure 1B. The good agreement between the FGR based predictions and the results of our simulations, specially at high temperatures, validates the methodology.

IV. ELECTRONIC TRANSPORT AND JOULE HEATING

Open-boundary transport simulations were performed employing the driven Liouville von Neumann (DLvN) equation.[47–50] In this approach, the charge is injected or removed in the lead regions through the inclusion of a driving term in the quantum Liouville equation, thus inducing a chemical potential imbalance between the electrodes. The speed at which the electron charge is exchanged at the leads is determined by a driving rate parameter Γ whose value can be established on the basis of different criteria or methodologies, depending on the computational implementation.[48,50,51] The extension of LvN+KE to quantum open boundary conditions gives:

$$\frac{\partial \rho}{\partial t} = \frac{1}{\mathrm{i}\hbar}[H_e, \rho] - \begin{bmatrix} \eta_1\rho_{11} - \Lambda_1 & \frac{\eta_1+\eta_2}{2}\rho_{12} & \cdots & \frac{\eta_1+\eta_n}{2}\rho_{1N} \\ \frac{\eta_2+\eta_1}{2}\rho_{21} & \eta_2\rho_{22} - \Lambda_2 & \cdots & \frac{\eta_2+\eta_N}{2}\rho_{2N} \\ \vdots & \vdots & \ddots & \vdots \\ \frac{\eta_N+\eta_1}{2}\rho_{N1} & \frac{\eta_N+\eta_2}{2}\rho_{N2} & \cdots & \eta_N\rho_{NN} - \Lambda_N \end{bmatrix} - \\ -\Gamma c^T \begin{bmatrix} \bar{\rho}_S - \bar{\rho}^0_S & \frac{1}{2}(\bar{\rho}_{SM} - \bar{\rho}^0_{SM}) & \bar{\rho}_{SD} - \bar{\rho}^0_{SD} \\ \frac{1}{2}(\bar{\rho}_{MS} - \bar{\rho}^0_{MS}) & 0 & \frac{1}{2}(\bar{\rho}_{MD} - \bar{\rho}^0_{MD}) \\ \bar{\rho}_{DS} - \bar{\rho}^0_{DS} & \frac{1}{2}(\bar{\rho}_{DM} - \bar{\rho}^0_{DM}) & \bar{\rho}_D - \bar{\rho}^0_D \end{bmatrix} c. \tag{22}$$

In the above expression, that we call DLvN+KE, the bar on the density matrix elements ($\bar{\rho}$) refers to the atomic representation, which enables to project the driving term (the last term on the right) on the different regions: Source, Drain, and Molecule, denoted with subindices S, D, and M respectively. c is the matrix of eigenvectors of the electronic system. In this way the density matrix can be projected from one representation to the other: $\rho = c^T\bar{\rho}c$. $\bar{\rho}^0$ is a reference density matrix which is constant in time and encodes the chemical potential on each lead. This density was constructed through the application of a potential $\pm V/2$ on

the Drain and the Source in the atomic representation. The eigenvectors and eigenvalues of this system were used to obtain the electron-phonon terms in the KE. During the dynamics, this potential was removed and the charge density, initially set equal to $\bar{\rho}^0$, flowed from the Source to the Drain across the Molecule.[50,52] In the present simulations a TB chain of 115 atoms was used, of which the 40 terminal atoms on each end were part of the leads, whilst the Molecule encompassed the remaining 35 atoms in the central region. Unless otherwise noted, the applied electric potential difference V was 1.0 eV, with a driving rate $\Gamma = 0.2$ fs^{-1}, corresponding to the value which maximizes the current for this system in the absence of electron-phonon coupling. Simulations were performed replacing 1, 3, 5, 9 or 15 atoms by Einstein oscillators, distributed next to each other in the center of the chain. All the EO had $M = 0.5$ amu, $\hbar\omega = 0.2$ eV, and $C = 1.0$ eV/. Phonon populations were evolved according to equation (8), starting from an initial temperature equal to zero for both electrons and phonons.

Figure 3A shows the current as a function of time for systems with different number of EO. As more oscillators are involved, the lower the stationary current, which results from the increased inelastic scattering. Indeed, after the initial transient, the current as a function of time shows a slight decrease, more prominent for larger numbers of EO: the signature of the concurrent heating of the oscillators. This heating can be seen in Figure 3B and increases the scattering rate experienced by the electrons. Overall, these results show that the DLvN+KE formulation qualitatively captures the Joule heating.

To get a quantitative assessment of the performance of our model, we discuss in what follows its description of Ohm's law. To this end, we consider that the system is in the

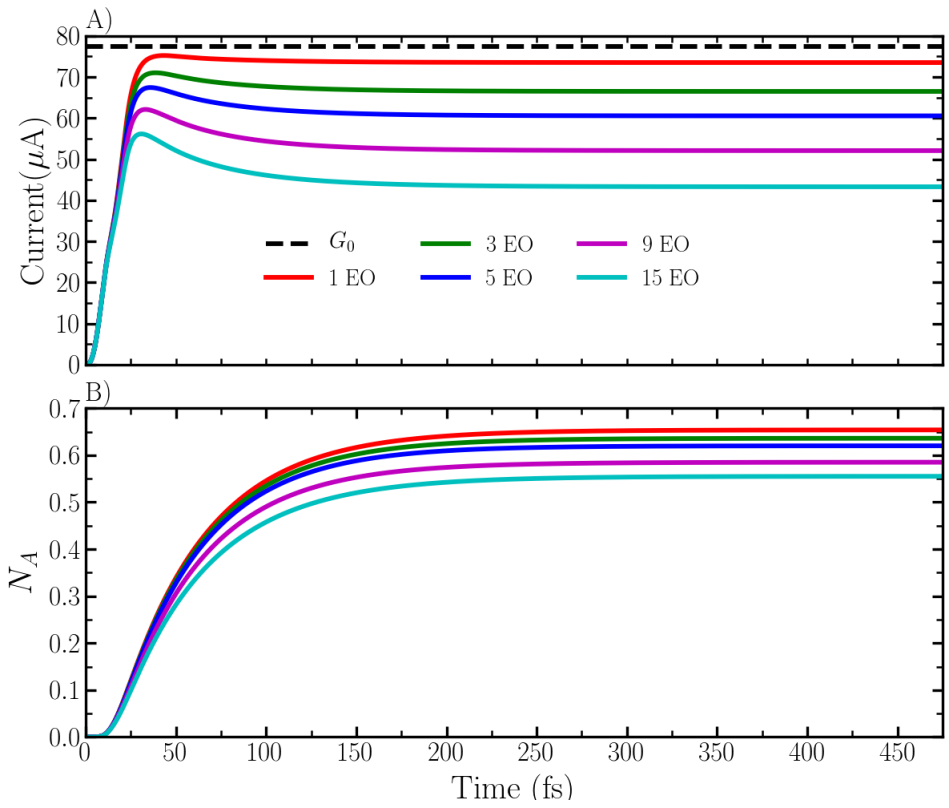

FIG. 3. A) Current as a function of time in an atomic wire with different number of Einstein oscillators, and initial temperature equal to zero. The dashed black line indicates the conductance quantum G_0=77.48 μA. B) Average population per Einstein oscillator as a function of time for the systems represented in (A).

diffusive regime. Then the resistance of a nanowire is given by[53]

$$R = r_0 \left(1 + \frac{L}{l_0}\right), \tag{23}$$

where $r_0 = \hbar\pi/e^2 = 0.0129$ V/μA, l_0 is the electron mean free path (EMFP), and L the length of the scatterer. The EMFP associated with a given scattering potential can be estimated perturbatively from FGR considering an infinite chain, in a similar way as the back-scattering decay time in equation (21):[54]

$$\frac{a}{l_0} = \frac{4C^2}{b^2}\frac{(N+1/2)\hbar}{M\omega}, \tag{24}$$

where a is the lattice parameter. To examine the resistance, transport simulations were carried out in the same system, but in this case with the thermalization of the phonons setting $\dot{N}(t) = 0$ and an initial temperature given by $kT = 0.136$ eV. The results of these calculations, presented in Figure 4, show that the stationary state is reached faster when the phonon occupancies are kept constant. The resistance, readily obtained as the ratio between the bias and the current, scales linearly with the number of EO, as predicted by equations (23) and (24). However, these values do not exactly agree with those calculated on the basis of FGR. This might be a consequence of the system moving beyond the quasi-stationary condition, outside the range of validity of DLvN+KE. In particular, a decrease in Γ provokes a drop in the current.[48–50,52] Figure 5 presents the dependence of the resistance with respect to the number of EO, for different driving rates. On one hand, a decrease in Γ may drive the system closer to the quasi-stationary premise. On the other, however, it results in an underestimation of the current, which explains the increase in the resistance. As a consequence of these effects, the agreement between the simulations and the FGR predictions appears to be better for intermediate Γ values.

To gain further insight on this behavior, Figure 6 focuses on the dependence of the EMFP on the coupling parameter C, on the oscillator mass, and on temperature, for different values of Γ. The trends are consistent with the above observation regardless of T, C, or M: the agreement with FGR improves as Γ becomes smaller, but then it deteriorates again. This result can be rationalized as follows. The KE is formulated in the basis of eigenstates of the finite system, but it is used in open-boundaries including the electrodes. As Γ becomes smaller, the former becomes a better approximation to the latter, and the description improves. (Indeed, the resistance per unit length, or the resistivity, given by the slope in Figure 5, improves systematically with decreasing Γ.) However, for small enough

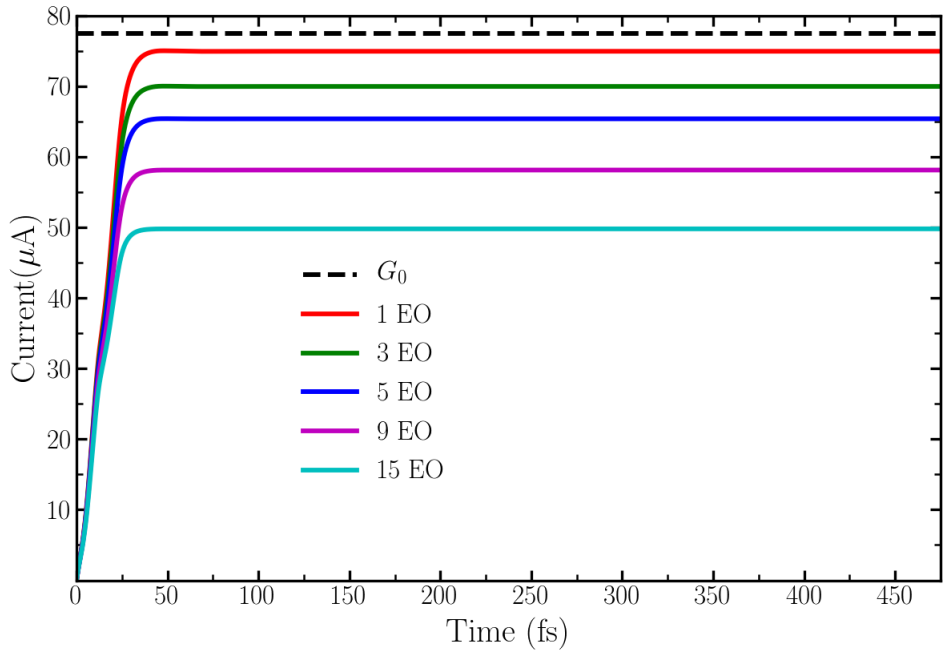

FIG. 4. Current as a function of time in an atomic wire with different number of Einstein oscillators, and thermalization of the phonons at kT= 0.136 eV. The dashed black line indicates the conductance quantum G_0=77.48 μA.

values of Γ, the ballistic regime of electron transport, assumed in the FGR calculation, is not valid any longer. For ballistic transport $\hbar \cdot \Gamma$ should be as small as possible but not smaller than the energy level spacing in the leads. In this way, larger reservoirs would allow for smaller values of Γ, at the expense of a higher computational cost.

A similar trend emerges when we consider the Joule heating for different driving rates. By assuming that in the absence of electron-phonon interaction the ballistic regime holds, and taking into consideration the conductance quantum $G_0 = 77.48\ \mu A/\mathrm{V}$, it is possible from the $I - V$ curves obtained with different Γ values, to associate a given current to a particular effective potential. Focusing on the case of only 1 EO, the injected population of phonons in the ballistic regime is expected to be such that (N+1/2)$\hbar\omega$ is equal to half of this effective potential. Figure 7 shows the relation of both quantities for different values of Γ.

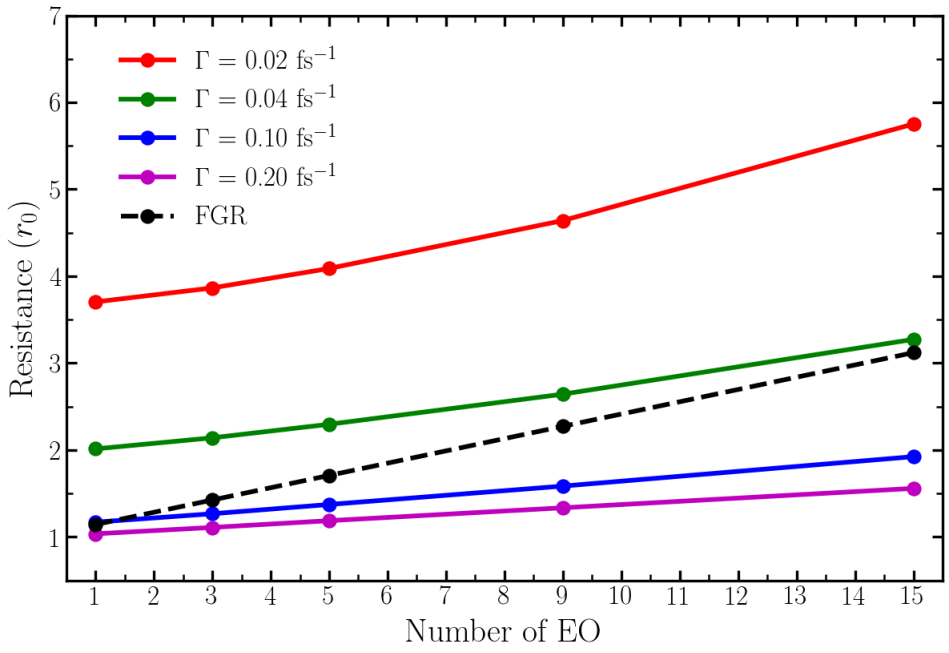

FIG. 5. Resistance as a function of the number of Einstein oscillators for different driving rates Γ, corresponding to the systems of Figure 4. The dashed line represents the resistances predicted from the Fermi golden rule.

Again, the results show that for intermediate values of the driving rate we get the expected behaviour. Noticeably, in this case the agreement would be reached for bigger Γ values than expected from the discussion in the previous paragraphs. This disagreement could be another consequence of leaving the ballistic regime, meaning that the phonon injection is more sensitive to the effect of the driving rate.

Very recently, a study on two-level and single-level biased molecular junctions has pointed out that under certain conditions the effective temperature may not be appropriate to characterize the nonequilibrium steady state of vibrations.[15] Instead, a nonthermal, coherent vibrational state associated with lower entropy and higher free energy may develop. It would be interesting to explore in further investigations how the present model performs in such a regime.

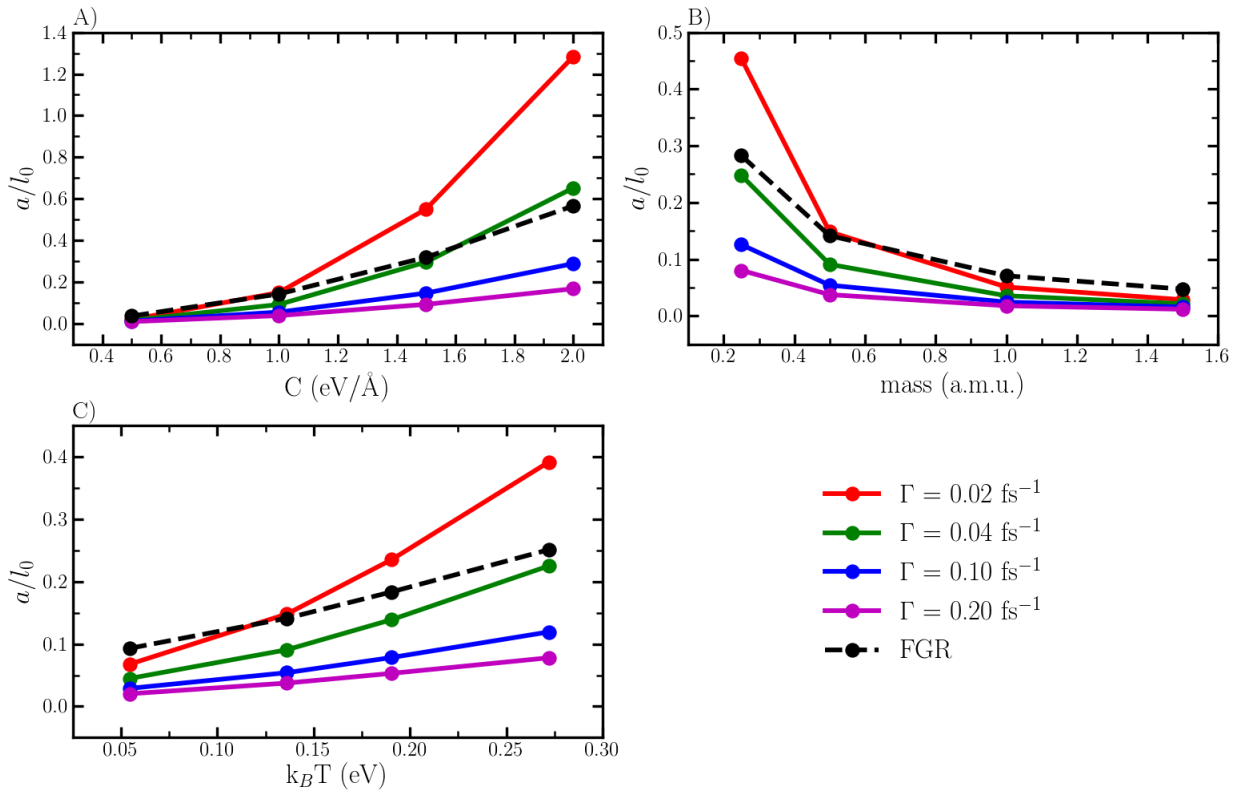

FIG. 6. Dependence of the electron mean free path (l_0) as a function of: A) the coupling term C; B) the oscillator mass; C) the temperature. Results corresponding to the atomic wire of Figure 4 with 15 Einstein oscillators and different values of Γ. Dashed lines represent the predictions based on the Fermi golden rule.

V. SUMMARY

In this work we have introduced the LvN+KE equation, that extends the scope of the Kinetic Model on which it is based, through the incorporation of coherence. Using a tight-binding Hamiltonian, this model was able to reproduce the broadening in the electronic spectrum of an atomic wire arising from the electron-phonon interaction. The results showed agreement with the predictions based on Fermi's Golden Rule.

Encouraged by these findings, the methodology was implemented in the context of the

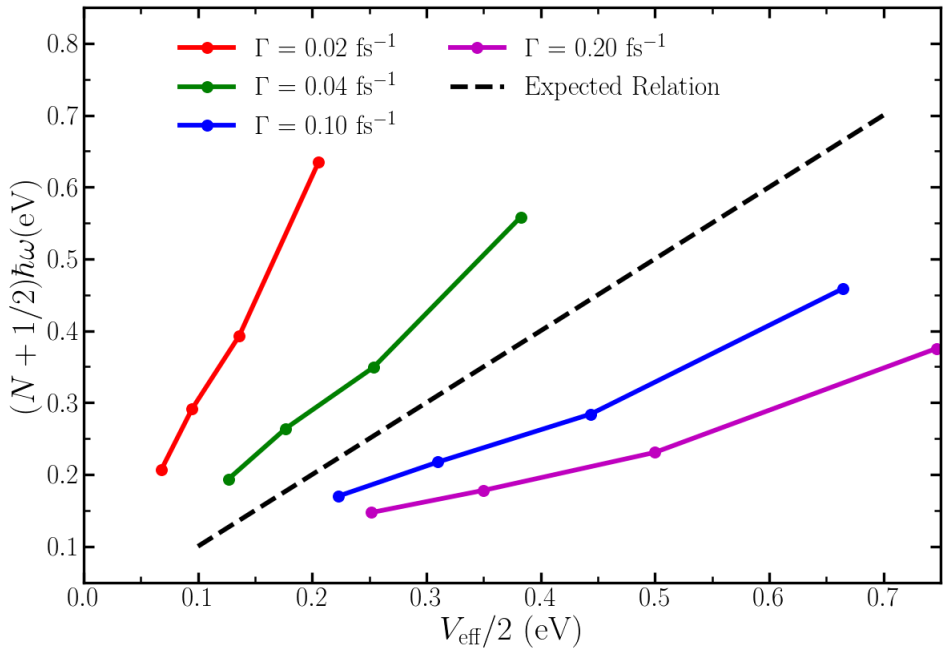

FIG. 7. Vibronic energy of the phonon population N in function of the effective potential (V_{eff}). In dashed black line is represented the expected relation between both quantities.

DLvN equation to study the effect of electron-phonon interactions on electron transport. The emerging approach, denoted as DLvN+KE, reproduces qualitatively the Joule heating. Moreover, the predicted trends are consistent with the microscopic Ohm's law, although the numerical results do not fully agree in this case with those calculated via the FGR. A possible explanation for this disagreement is that the approximation of considering the eigenstates of the finite system to build KE, is not appropriate for the open-boundary description. Intermediate values of Γ improve the agreement but on the other hand tend to break the ballistic regime assumed in the FGR calculation. The simplicity, numerical speed, and flexibility of this formalism make it suitable for its implementation in *ab initio* calculations. Work in this direction is underway.

ACKNOWLEDGMENTS

We thank Myrta Grüning for helpful discussions. This work has been funded by the European Union's Horizon 2020 research and innovation programme through the project ATLANTIC under grant agreement No 823897, and by the Agencia Nacional de Promoción Científica y Tecnológica de Argentina (PICT 2015-2761 and PICT 2016-3167). APH acknowledges support from the Thomas Young Centre under Grant No. TYC-101.

DATA AVAILABILITY STATEMENT

The data that support the findings of this study are available from the corresponding author upon reasonable request.

Appendix: The σ parameter

The parameter σ in equation (8) plays an important role in the dynamics and in the final temperature of the fermionic and bosonic subsystems. Figure 8 shows the evolution of the electronic population for an atomic wire with initial electronic temperatue $kT_e = 0.4$ eV and vibrational temperature $kT_{vib} = 0.1$ eV. The oscillator frequency was $\omega_j = 0.12$ eV$/\hbar$ for all the bosons. High σ values provoke an unphysical heating of the electrons. Too small values, on the other hand, induce jumps or discontinuities between states, specially around the Fermi level, possibly related with numerical unstabilities.

To calibrate this parameter, the phonon population was fixed during the dynamics, thus providing a thermostat for the electrons. In this way the effect of σ on the final electronic temperature could be assessed, see Figure 9. The same procedure was carried out but fixing the electronic populations, to determine the influence of σ on the equilibrium phonon temperature. The optimal σ will be the one for which the final temperatures are the same

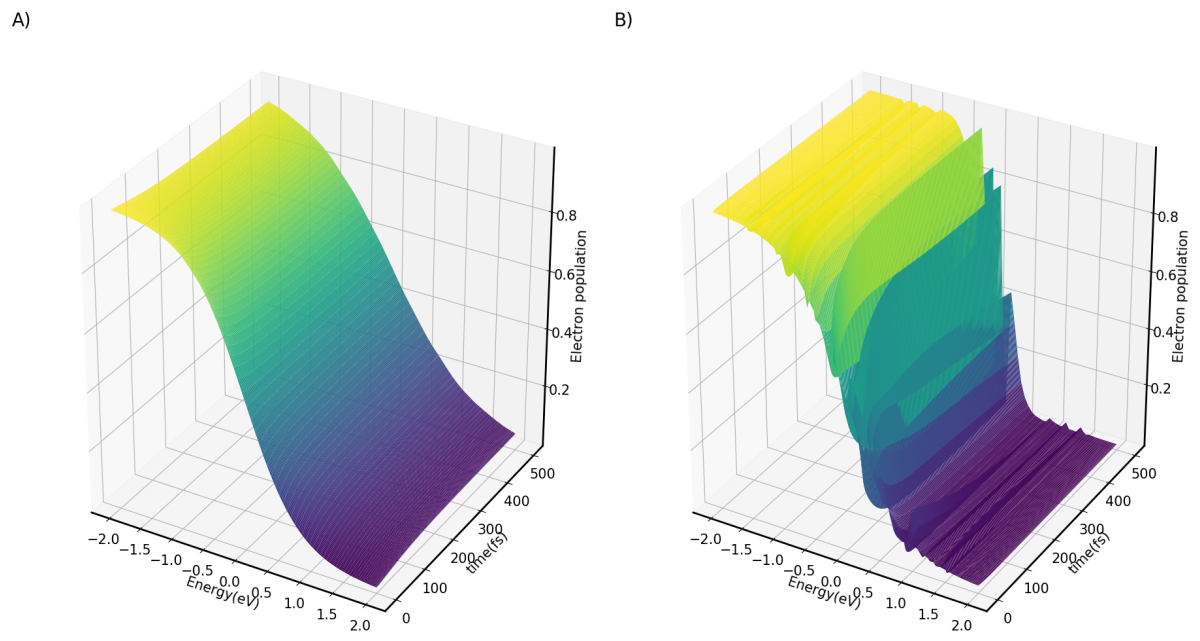

FIG. 8. Evolution of the electronic occupancies in an atomic wire with initial temperatures kT_e = 0.4 eV and kT_{vib} = 0.1 eV. A) $\sigma = 0.25$ eV and B) $\sigma = 0.0002$ eV.

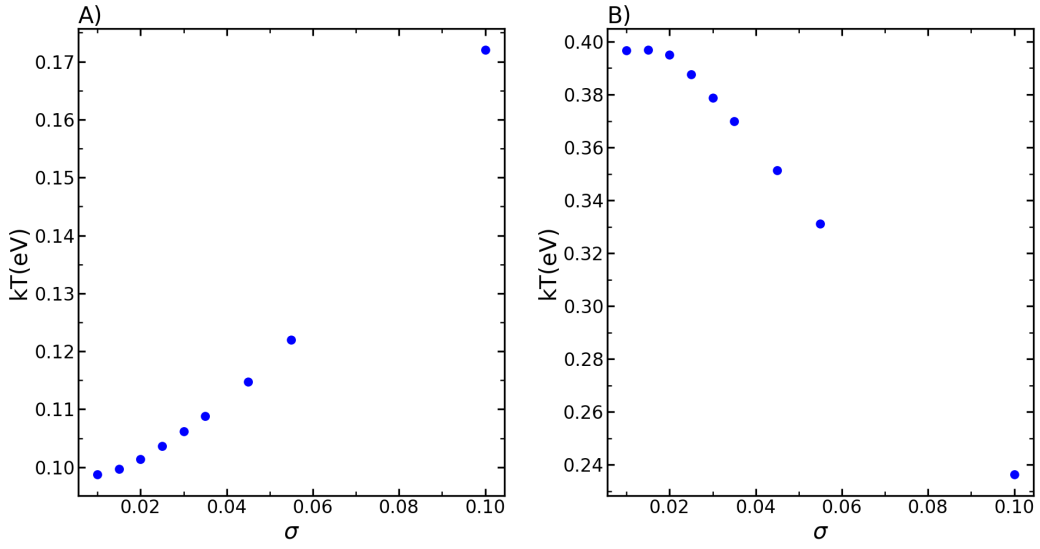

FIG. 9. Effect of the σ parameter on the equilibrium temperature of an atomic wire: A) final temperature of the electrons in a thermalized phonon bath with kT_{vib}=0.1 eV; B) final temperature of the phonons in a thermalized electron bath with kT_e = 0.4 eV.

for both subsystems, i.e., $kT_e = kT_{vib}$. The final electron temperatures were calculated as the inverse slope of the function $\log(1/\rho_\alpha - 1)$ plotted against the electronic energy once the stationary state was reached. The phonon temperatures were similarly obtained, using the function $\log(1/N_j + 1)$ instead. The results in Figure 9 show that an appropriate value for σ is in the present case in the region of 0.015 eV. This value reproduces correctly the temperature of both subsystem at the end of the dynamics.

REFERENCES

[1]F. Giustino, "Electron-phonon interactions from first principles," Reviews of Modern Physics **89**, 015003 (2017).

[2]M. Galperin, M. A. Ratner, and A. Nitzan, "Molecular transport junctions: vibrational effects," Journal of Physics: Condensed Matter **19**, 103201 (2007).

[3]N. J. Tao, "Electron transport in molecular junctions," in *Nanoscience And Technology: A Collection of Reviews from Nature Journals* (2010) pp. 185–193.

[4]T. N. Todorov, J. Hoekstra, and A. P. Sutton, "Current-induced embrittlement of atomic wires," Physical Review Letters **86**, 3606–3609 (2001).

[5]Z. Chen and R. Sorbello, "Local heating in mesoscopic systems," Physical Review B **47**, 13527 (1993).

[6]T. Frederiksen, M. Brandbyge, N. Lorente, and A.-P. Jauho, "Inelastic scattering and local heating in atomic gold wires," Physical Review Letters **93**, 256601 (2004).

[7]A. P. Horsfield, D. Bowler, A. Fisher, T. N. Todorov, and M. Montgomery, "Power dissipation in nanoscale conductors: classical, semi-classical and quantum dynamics," Journal of Physics: Condensed Matter **16**, 3609 (2004).

[8]L. A. Zotti, M. Bürkle, F. Pauly, W. Lee, K. Kim, W. Jeong, Y. Asai, P. Reddy, and J. C. Cuevas, "Heat dissipation and its relation to thermopower in single-molecule junctions," New Journal of Physics **16**, 015004 (2014).

[9]T. N. Todorov, D. Dundas, J.-T. Lü, M. Brandbyge, and P. Hedegård, "Current-induced forces: a simple derivation," European Journal of Physics **35**, 065004 (2014).

[10]T. Gunst, T. Markussen, K. Stokbro, and M. Brandbyge, "First-principles method for electron-phonon coupling and electron mobility: Applications to two-dimensional materi-

als," Physical Review B **93**, 035414 (2016).

[11]V. Rizzi, T. N. Todorov, J. J. Kohanoff, and A. A. Correa, "Electron-phonon thermalization in a scalable method for real-time quantum dynamics," Physical Review B **93**, 024306 (2016).

[12]W. Dou and J. E. Subotnik, "Perspective: How to understand electronic friction," The Journal of Chemical Physics **148**, 230901 (2018).

[13]L. Kantorovich, "Nonadiabatic dynamics of electrons and atoms under nonequilibrium conditions," Physical Review B **98**, 014307 (2018).

[14]J.-T. Lü, S. Leitherer, N. R. Papior, and M. Brandbyge, "Ab initio current-induced molecular dynamics," Physical Review B **101**, 201406 (2020).

[15]T. Wang, L.-L. Nian, and J.-T. Lü, "Nonthermal vibrations in biased molecular junctions," Physical Review E **102**, 022127 (2020).

[16]G. Mahan, *Many-Particle Physics*, 3rd ed. (Kluwer Academic, 2000).

[17]X. Gonze, D. C. Allan, and M. P. Teter, "Dielectric tensor, effective charges, and phonons in α-quartz by variational density-functional perturbation theory," Physical Review Letters **68**, 3603–3606 (1992).

[18]S. Baroni, S. de Gironcoli, A. D. Corso, , and P. Giannozzi, "Phonons and related crystal properties from density-functional perturbation theory," Reviews of Modern Physics **73**, 515–562 (2001).

[19]D. Marx and J. Hutter, *Ab Initio Molecular Dynamics* (Cambridge University Press, Cambridge, UK, 2009).

[20]M. D. Hack and D. G. Truhlar, "Nonadiabatic trajectories at an exhibition," The Journal of Physical Chemistry A **104**, 7917–7926 (2000).

[21]J. C. Tully, "Perspective: Nonadiabatic dynamics theory," The Journal of Chemical Physics

137, 22A301 (2012).

[22]M. Persico and G. Granucci, "An overview of nonadiabatic dynamics simulations methods, with focus on the direct approach versus the fitting of potential energy surfaces," Theoretical Chemistry Accounts **133**, 1526 (2014).

[23]F. Ramírez, G. D. Mirón, M. C. G. Lebrero, and D. A. Scherlis, "Qm–mm ehrenfest dynamics from first principles: photodissociation of diazirine in aqueous solution," Theoretical Chemistry Accounts **137**, 124 (2018).

[24]J. E. Subotnik, A. Jain, B. Landry, A. Petit, W. Ouyang, and N. Bellonzi, "Understanding the surface hopping view of electronic transitions and decoherence," Annual Review of Physical Chemistry **67**, 387–417 (2016).

[25]A. P. Horsfield, D. Bowler, A. Fisher, T. N. Todorov, and C. G. Sánchez, "Beyond ehrenfest: correlated non-adiabatic molecular dynamics," Journal of Physics: Condensed Matter **16**, 8251 (2004).

[26]A. P. Horsfield, D. Bowler, A. Fisher, T. N. Todorov, and C. G. Sánchez, "Correlated electron–ion dynamics: the excitation of atomic motion by energetic electrons," Journal of Physics: Condensed Matter **17**, 4793 (2005).

[27]V. Rizzi, T. N. Todorov, and J. J. Kohanoff, "Inelastic electron injection in a water chain," Scientific Reports **7**, 1–9 (2017).

[28]M. Head-Gordon and J. C. Tully, "Molecular dynamics with electronic frictions," The Journal of Chemical Physics **103**, 10137–10145 (1995).

[29]N. Bode, S. V. Kusminskiy, R. Egger, and F. von Oppen, "Scattering theory of current-induced forces in mesoscopic systems," Physical Review Letters **107**, 036804 (2011).

[30]W. Dou, A. Nitzan, and J. E. Subotnik, "Frictional effects near a metal surface," The Journal of Chemical Physics **143**, 054103 (2015).

[31]W. Dou and J. E. Subotnik, "A many-body states picture of electronic friction: The case of multiple orbitals and multiple electronic states," The Journal of Chemical Physics **145**, 054102 (2016).

[32]M. Askerka, R. J. Maurer, V. S. Batista, and J. C. Tully, "Role of tensorial electronic friction in energy transfer at metal surfaces," Physical Review Letters **116**, 217601 (2016).

[33]W. Dou, G. Miao, and J. E. Subotnik, "Born-oppenheimer dynamics, electronic friction, and the inclusion of electron-electron interactions," Physical Review Letters **119**, 046001 (2017).

[34]F. Chen, K. Miwa, and M. Galperin, "Current-induced forces for nonadiabatic molecular dynamics," The Journal of Physical Chemistry A **123**, 693–701 (2019).

[35]W. Schäfer and M. Wegener, *Semiconductor Optics and Transport Phenomena* (Springer, 2002).

[36]H. Haug and S. W. Koch, *Quantum Theory of the Optical and Electronic Properties of Semiconductors*, 4th ed. (World Scientific, 2004).

[37]H. Haug and A.-P. Jauho, *Quantum Kinetics in Transport and Optics of Semiconductors*, 2nd ed. (Springer, 2008).

[38]E. J. McEniry, T. Frederiksen, T. N. Todorov, D. Dundas, and A. P. Horsfield, "Inelastic quantum transport in nanostructures: The self-consistent born approximation and correlated electron-ion dynamics," Phys. Rev. B **78**, 035446 (2008).

[39]T. N. Todorov and A. P. Horsfield, "Multiple-probe electronic open boundaries with bad contacts," Physical Review B **99**, 045415 (2019).

[40]K. Burke, R. Car, and R. Gebauer, "Density functional theory of the electrical conductivity of molecular devices," Physical Review Letters **94**, 146803 (2005).

[41]A. O. Govorov and H. Zhang, "Kinetic density functional theory for plasmonic nanos-

tructures: breaking of the plasmon peak in the quantum regime and generation of hot electrons," The Journal of Physical Chemistry C **119**, 6181–6194 (2015).

[42]M. Montgomery and T. Todorov, "Electron–phonon interaction in atomic-scale conductors: Einstein oscillators versus full phonon modes," Journal of Physics: Condensed Matter **15**, 8781 (2003).

[43]M. Montgomery and T. Todorov, "Erratum: Electron–phonon interaction in atomic-scale conductors: Einstein oscillators versus full phonon modes," Journal of Physics: Condensed Matter **16**, 6819 (2004).

[44]K. Yabana and G. Bertsch, "Time-dependent local-density approximation in real time," Physical Review B **54**, 4484 (1996).

[45]H. Chen, J. M. McMahon, M. A. Ratner, and G. C. Schatz, "Classical electrodynamics coupled to quantum mechanics for calculation of molecular optical properties: a rt-tddft/fdtd approach," The Journal of Physical Chemistry C **114**, 14384–14392 (2010).

[46]U. N. Morzan, F. F. Ramírez, M. B. Oviedo, C. G. Sánchez, D. A. Scherlis, and M. C. G. Lebrero, "Electron dynamics in complex environments with real-time time dependent density functional theory in a qm-mm framework," The Journal of Chemical Physics **140**, 164105 (2014).

[47]A. P. Horsfield, D. Bowler, and A. Fisher, "Open-boundary ehrenfest molecular dynamics: towards a model of current induced heating in nanowires," Journal of Physics: Condensed Matter **16**, L65 (2004).

[48]C. G. Sánchez, M. Stamenova, S. Sanvito, D. Bowler, A. P. Horsfield, and T. N. Todorov, "Molecular conduction: Do time-dependent simulations tell you more than the landauer approach?" The Journal of Chemical Physics **124**, 214708 (2006).

[49]T. Zelovich, L. Kronik, and O. Hod, "State representation approach for atomistic time-

dependent transport calculations in molecular junctions," Journal of Chemical Theory and Computation **10**, 2927–2941 (2014).

[50]U. N. Morzan, F. F. Ramírez, M. C. González Lebrero, and D. A. Scherlis, "Electron transport in real time from first-principles," The Journal of Chemical Physics **146**, 044110 (2017).

[51]T. Zelovich, T. Hansen, Z.-F. Liu, J. B. Neaton, L. Kronik, and O. Hod, "Parameter-free driven liouville-von neumann approach for time-dependent electronic transport simulations in open quantum systems," The Journal of Chemical Physics **146**, 092331 (2017).

[52]C. M. Bustamante, F. F. Ramirez, and D. A. S. Cristián G Sánchez, "Multiscale approach to electron transport dynamics," The Journal of Chemical Physics **151**, 084105 (2019).

[53]T. Todorov, "Calculation of the residual resistivity of three-dimensional quantum wires," Physical Review B **54**, 5801 (1996).

[54]V. Rizzi, *Real-Time Quantum Dynamics of Electron–Phonon Systems* (Springer, 2018).